Bifunctional Biomass-Derived Additive for Constructing a Hybrid SEI Layer to Enhance the Cycling Stability of Aqueous Zinc-Ion Batteries Under High Current Densities

Pengcheng Song[a], Zihan Wang[a], Wenxuan Liu[a], Heshun Geng[a], Yusheng Wu[a], Fang Hu[a*], Kai Zhu[b*]

[a] Shenyang University of Technology, College of Materials Science and Engineering, Shenyang Key Laboratory of Advanced Energy Materials and Renewable Resources, Shenyang 110870, Liaoning, China

[b] Key Laboratory of Superlight Materials and Surface Technology of Ministry of Education, College of Materials Science and Chemical Engineering, Harbin Engineering University, Harbin 150010, Heilongjiang, China

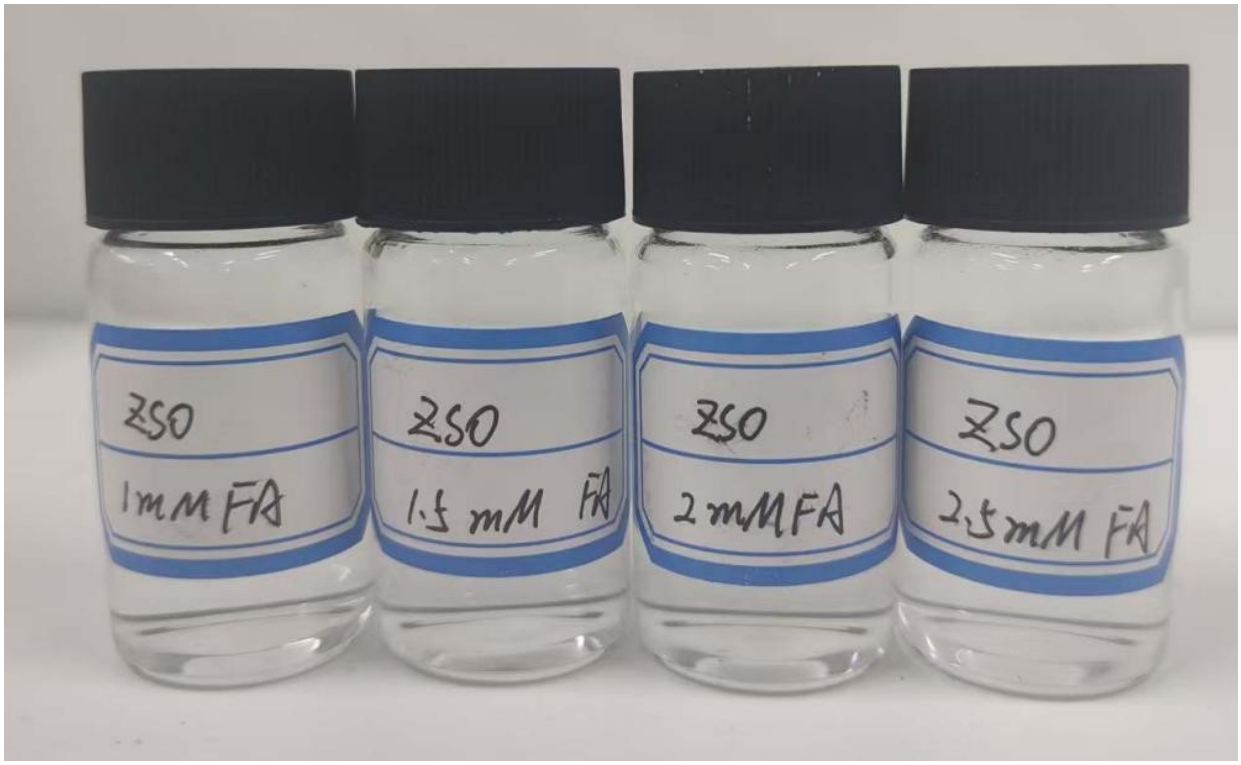

Figure S1: Electrolytes prepared with different concentrations of FA.

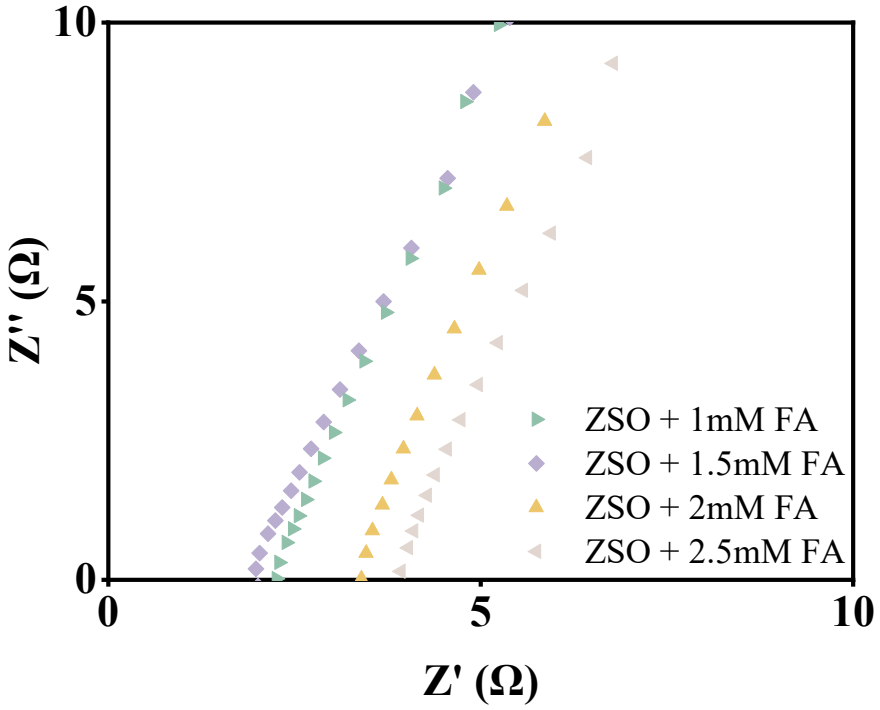

Figure S2: Nyquist plots of electrolytes with different concentrations of FA.

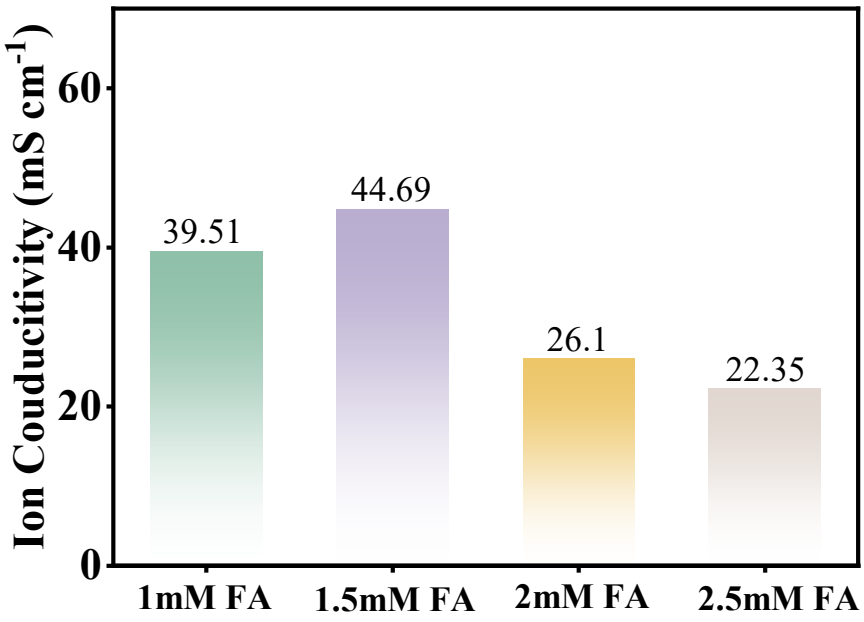

Figure S3: Corresponding conductivity.

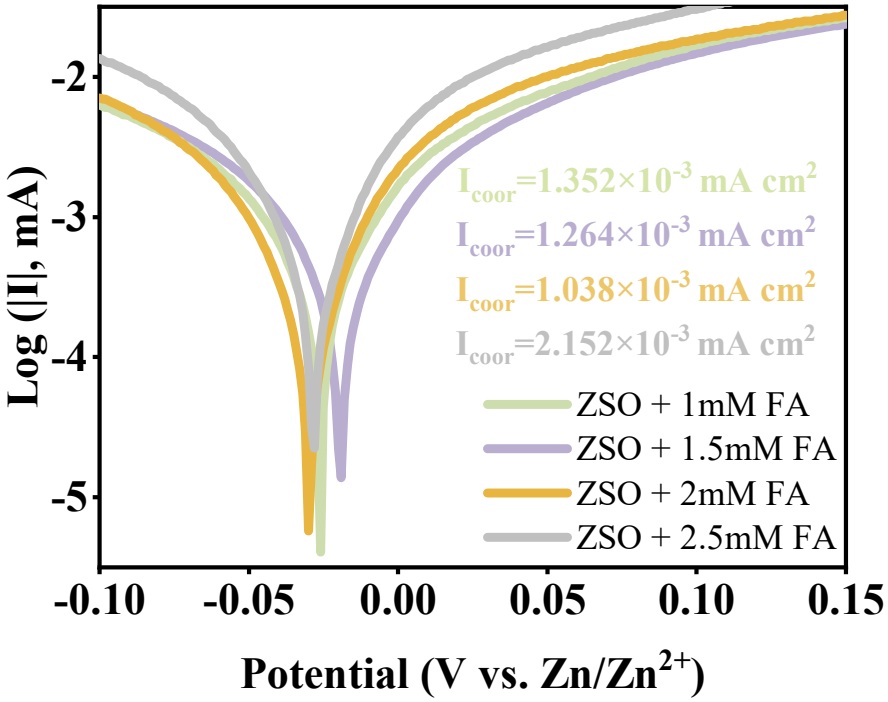

Figure S4: Tafel plots of electrolytes with different FA concentrations.

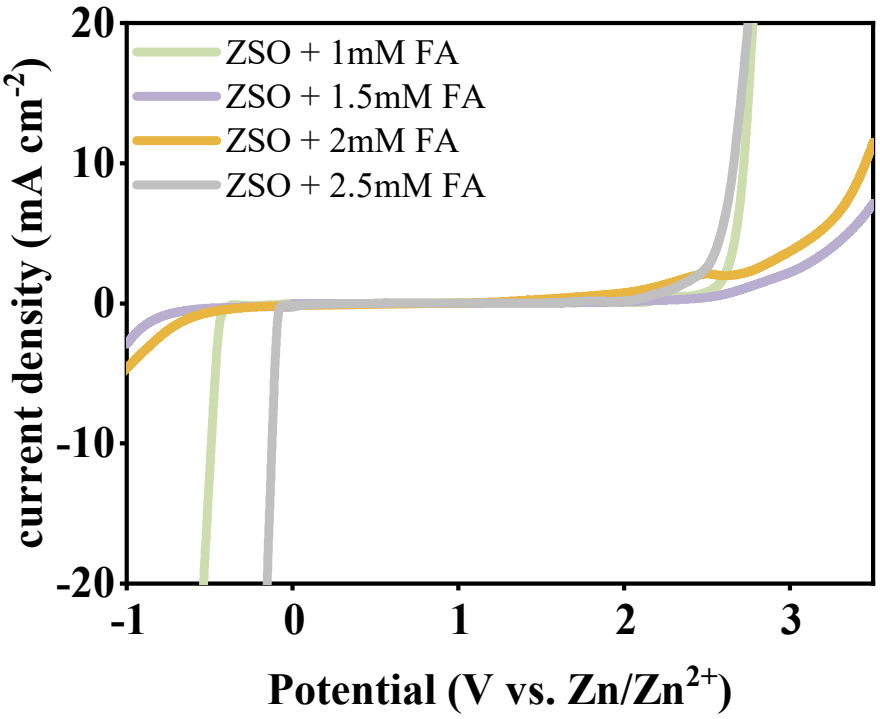

Figure S5: LSV curves of electrolytes with different FA concentrations.

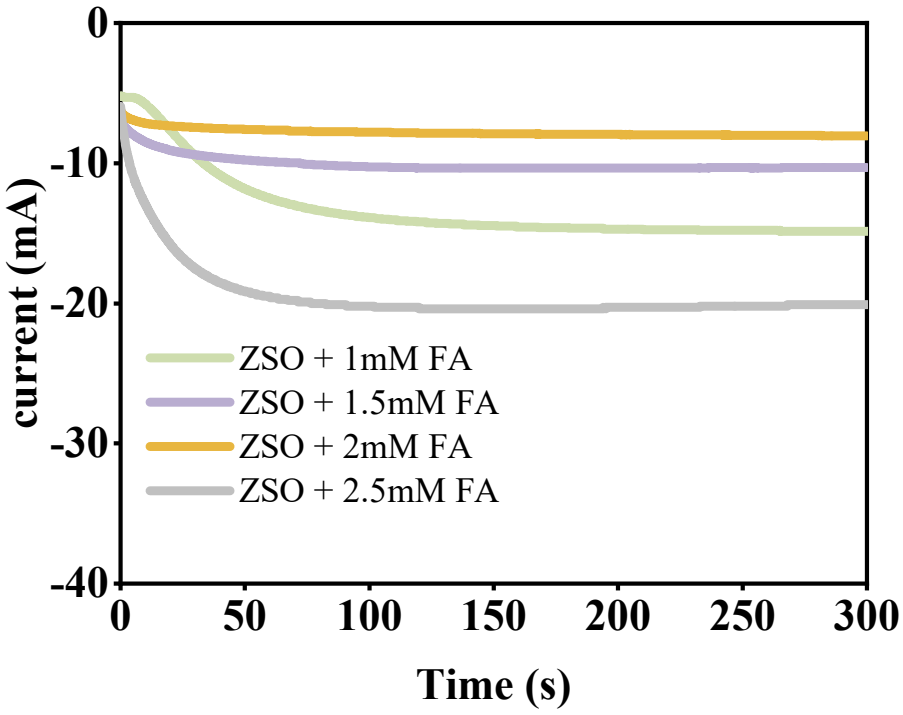

Figure S6: CA curves of electrolytes with different FA concentrations.

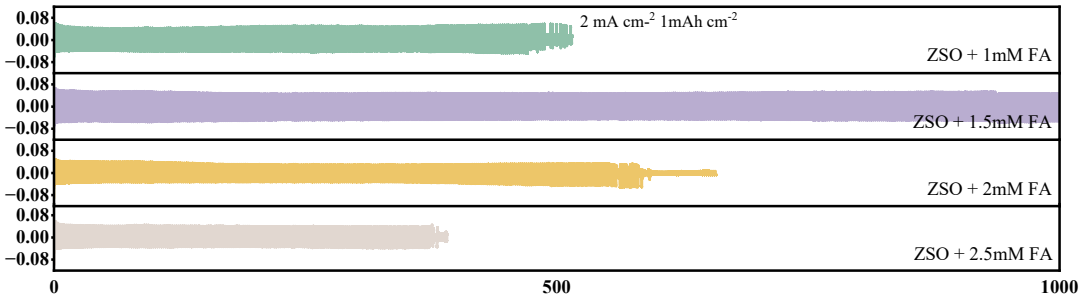

Figure S7: Cycling performance tests of Zn//Zn symmetric cells assembled with electrolytes of different FA concentrations.

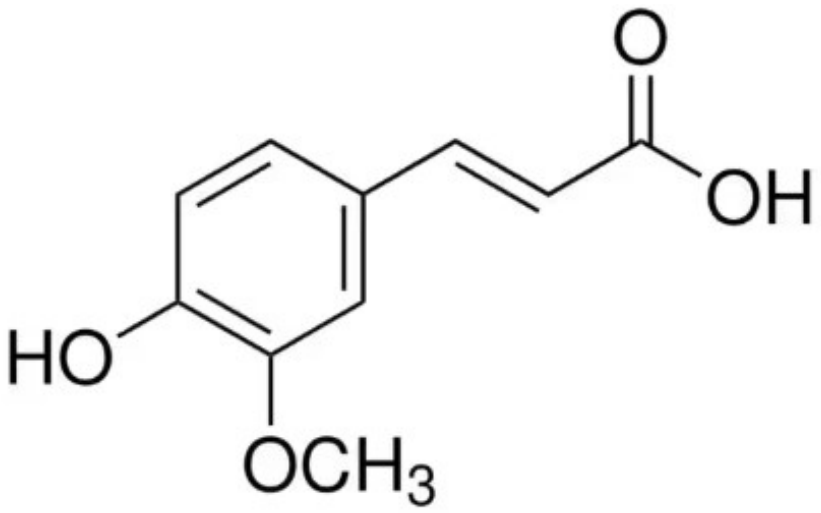

Figure S8: Chemical structure of FA.

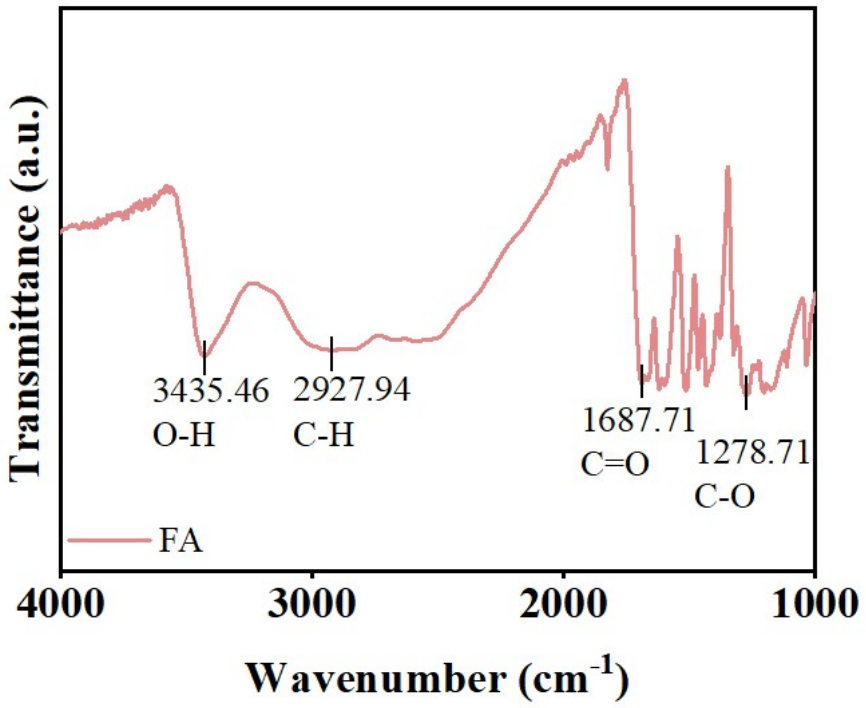

Figure S9: FTIR spectrum of FA.

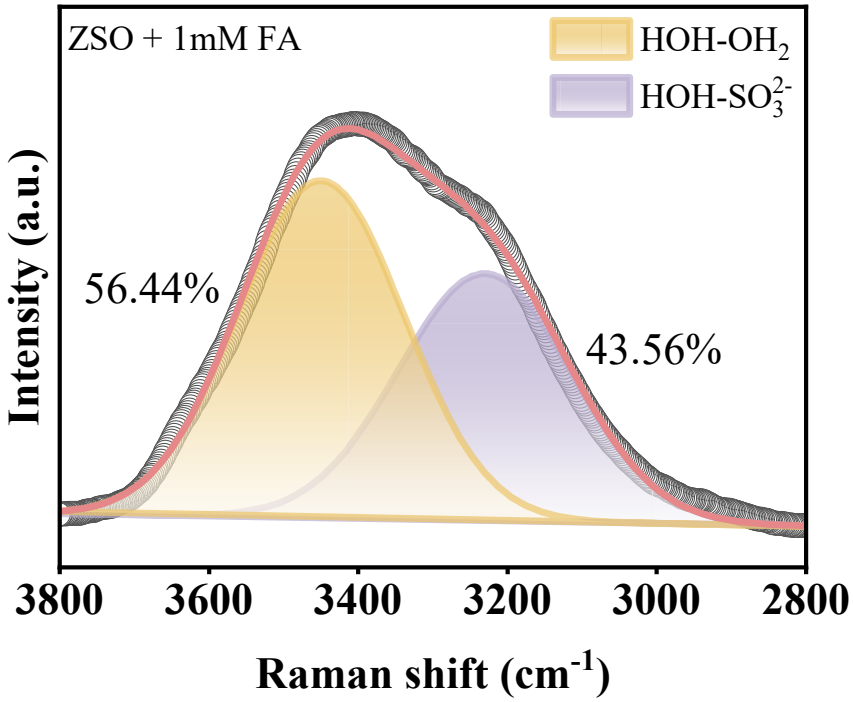

Figure S10: Raman Spectrum of the ZSO + 1 mM FA Electrolyte.

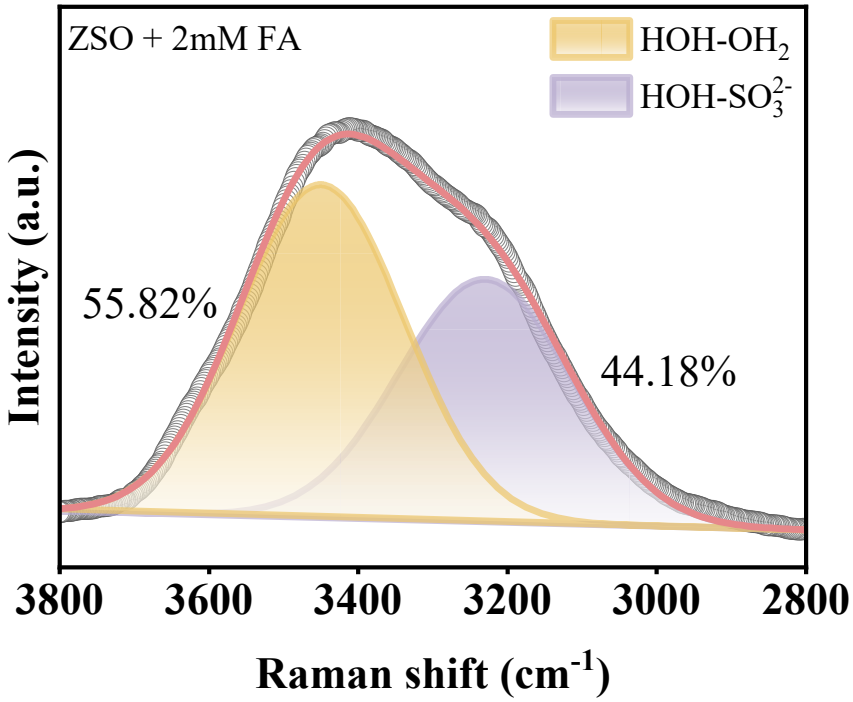

Figure S11: Raman Spectrum of the ZSO + 2 mM FA Electrolyte.

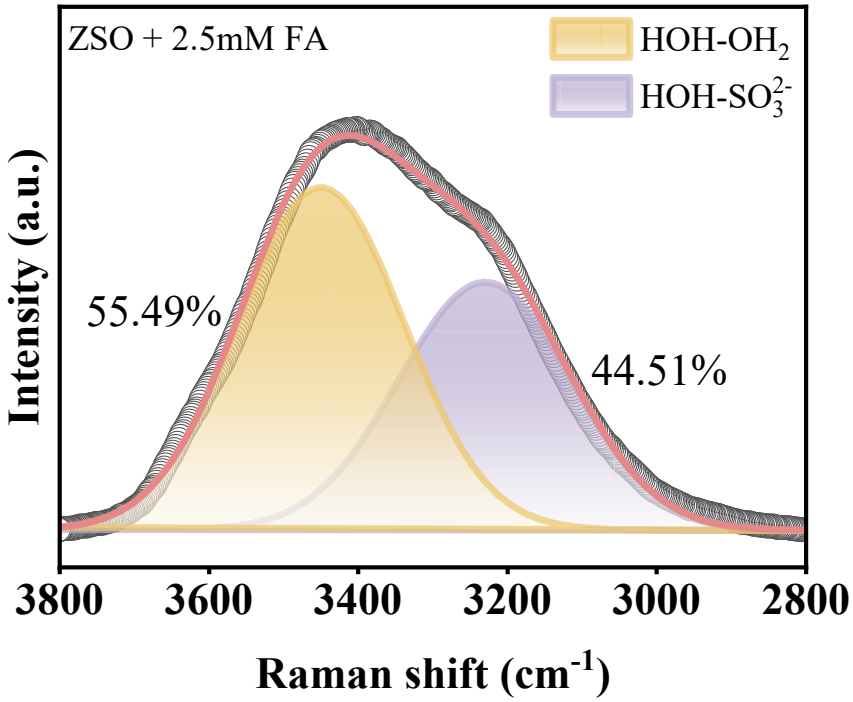

Figure S12: Raman Spectrum of the ZSO + 2.5 mM FA Electrolyte.

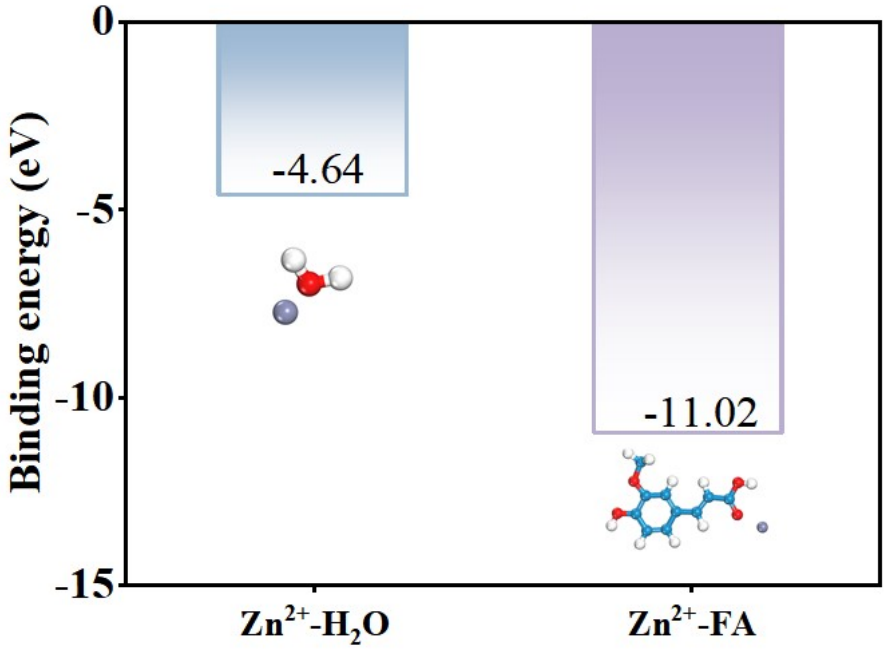

Figure S13: Binding energies of H_2O, and H_2O-FA molecules.

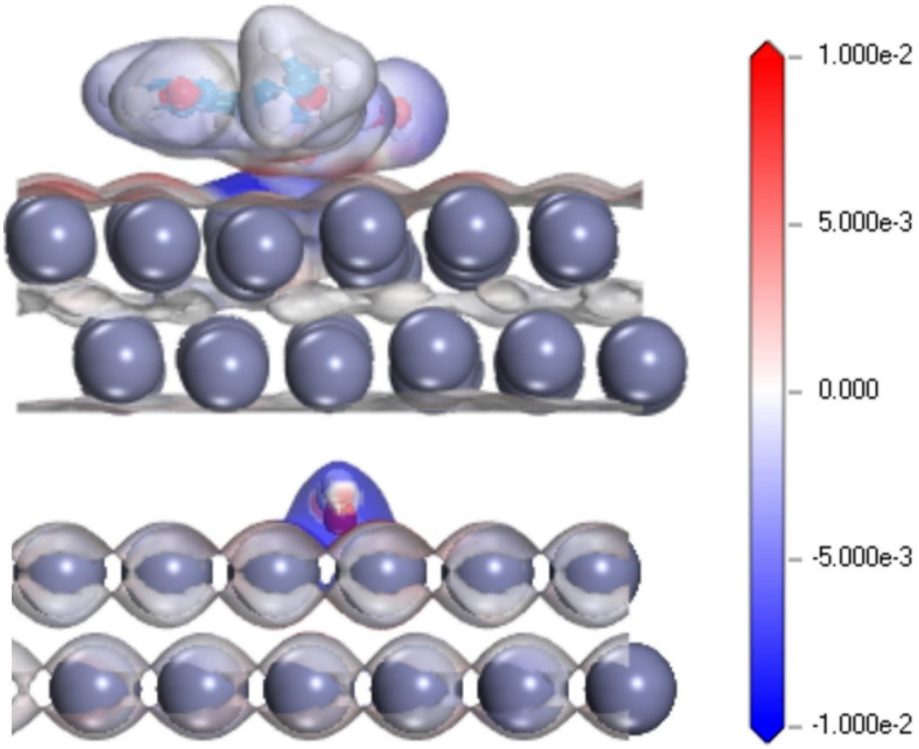

Figure S14: Charge density difference of Zn foil containing FA and H_2O molecules.

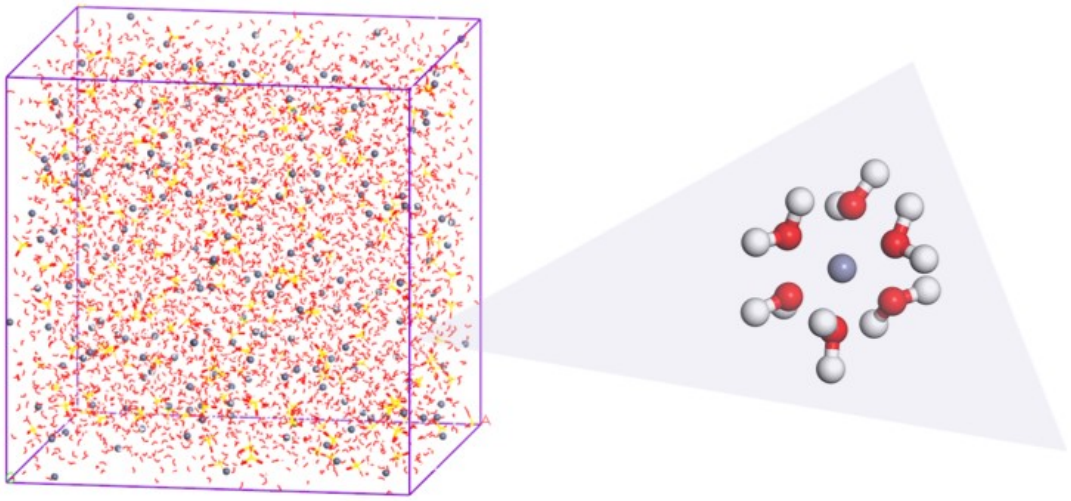

Figure S15: MD snapshots and schematic diagrams of the solvation structure of ZSO.

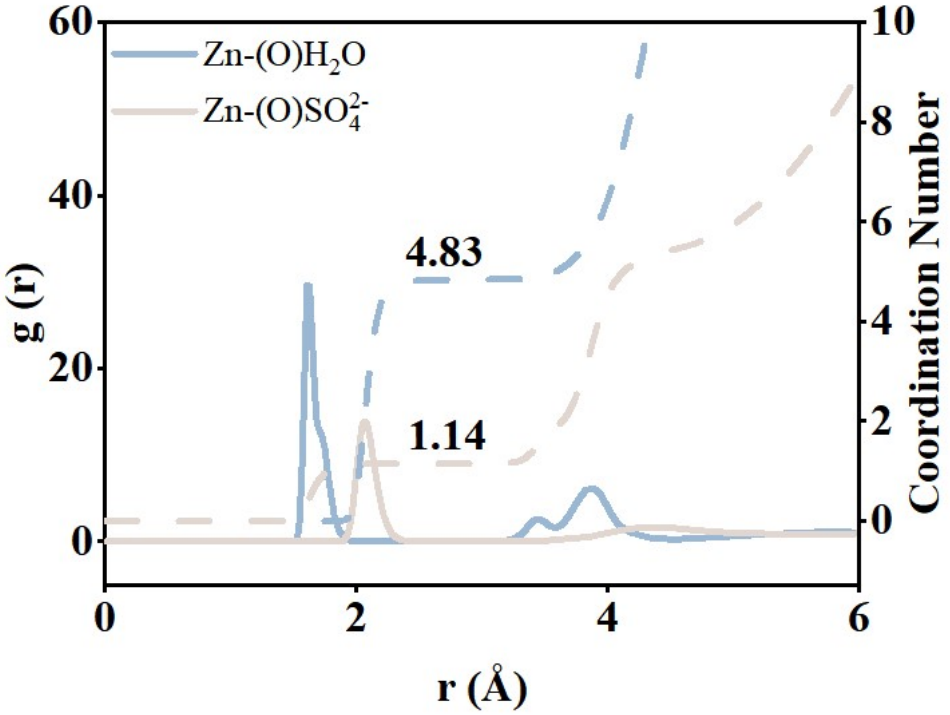

Fig. S16: Radial distribution function of ZSO.

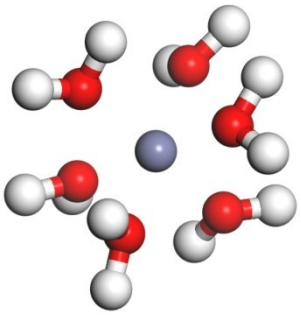

ΔE_{solv}=-0.204829Ha

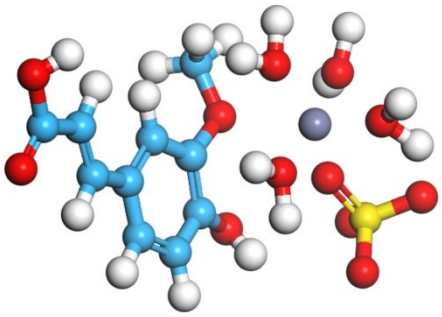

ΔE_{solv}=-2.424139Ha

Figure S17: Comparison of solvation energies

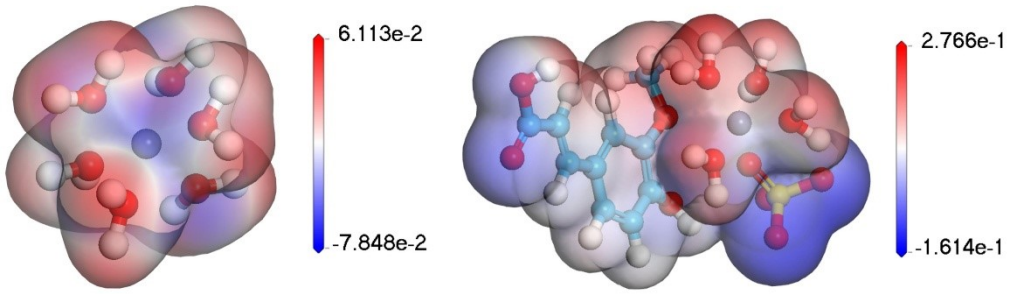

Figure S18: Comparison of electrostatic potential energies

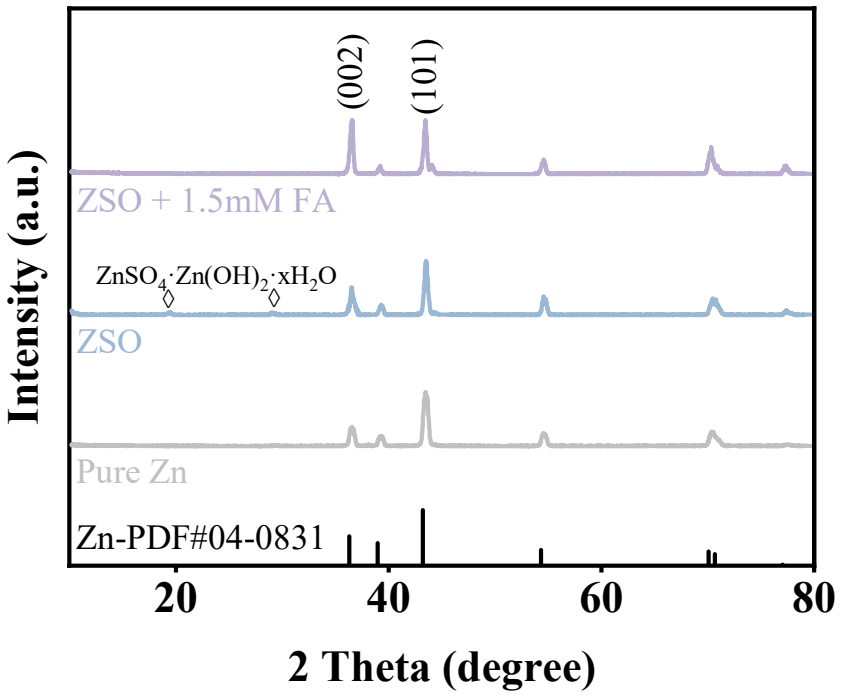

Figure S19: XRD patterns of zinc foils after 7-day immersion.

Figure S20: Thickness comparison of Zn symmetric cells before and after cycling.

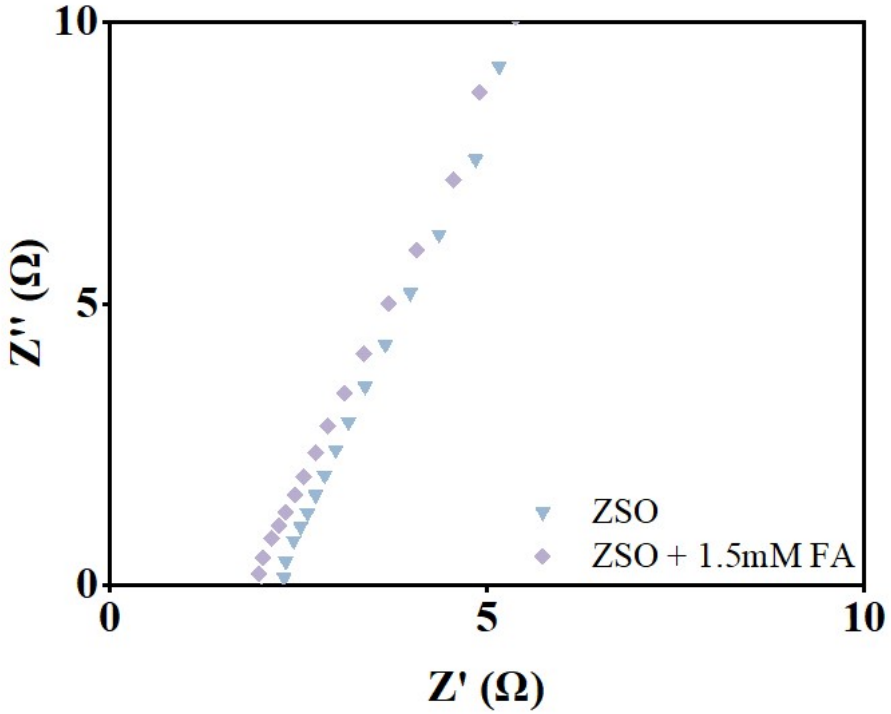

Figure S21: EIS plots of ZSO and ZSO + 1.5 mM FA electrolytes.

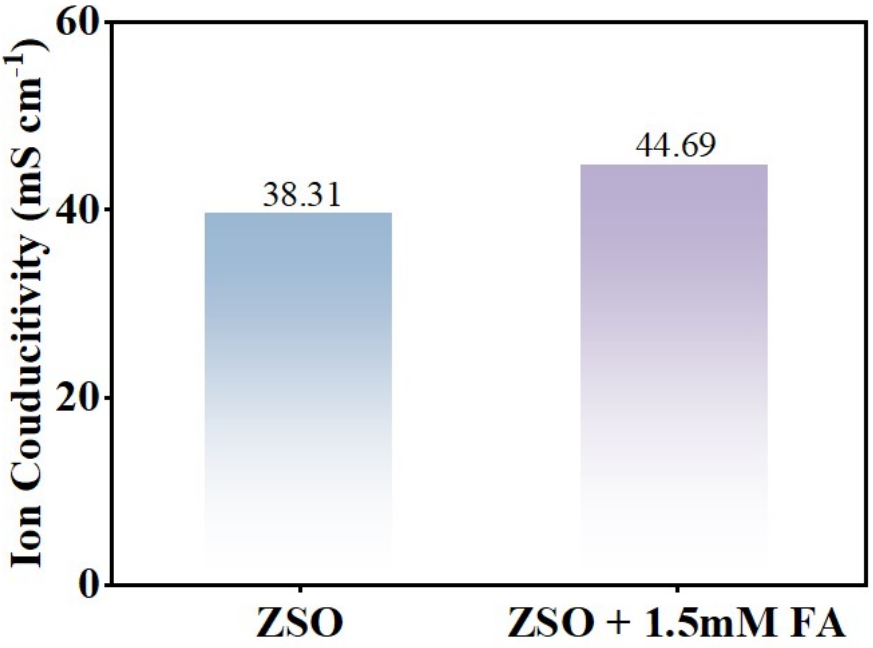

Figure S22: Calculated ionic conductivity.

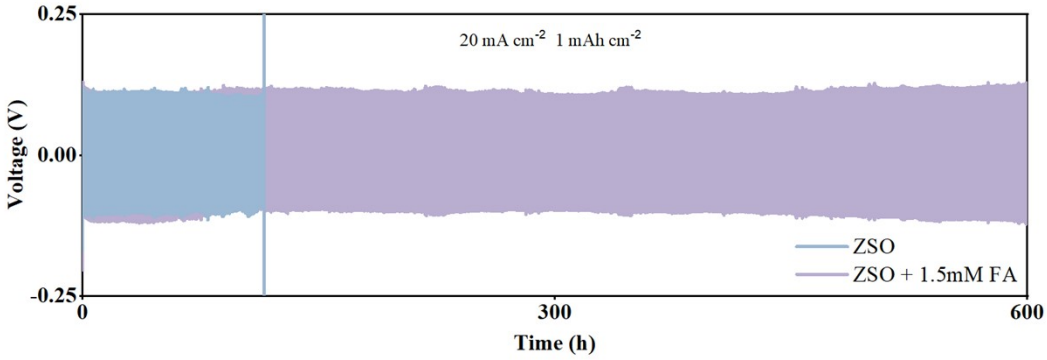

Figure S23: Long-term cycling performance at 20 mA cm^{-2} and 1 mAh cm^{-2}.

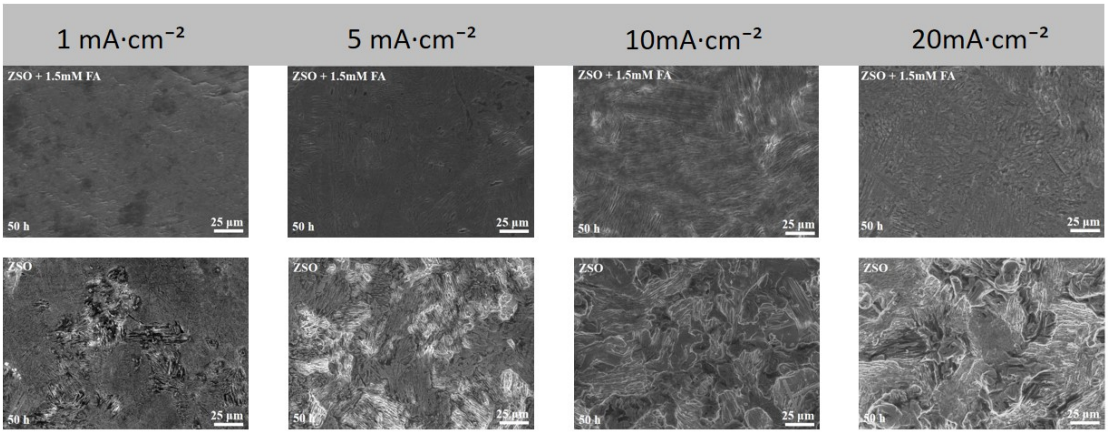

Figure S24: SEM images of zinc anode surfaces at different current densities (1 mA cm^{-2}, 5 mA cm^{-2}, 10 mA cm^{-2} and 20 mA cm^{-2})

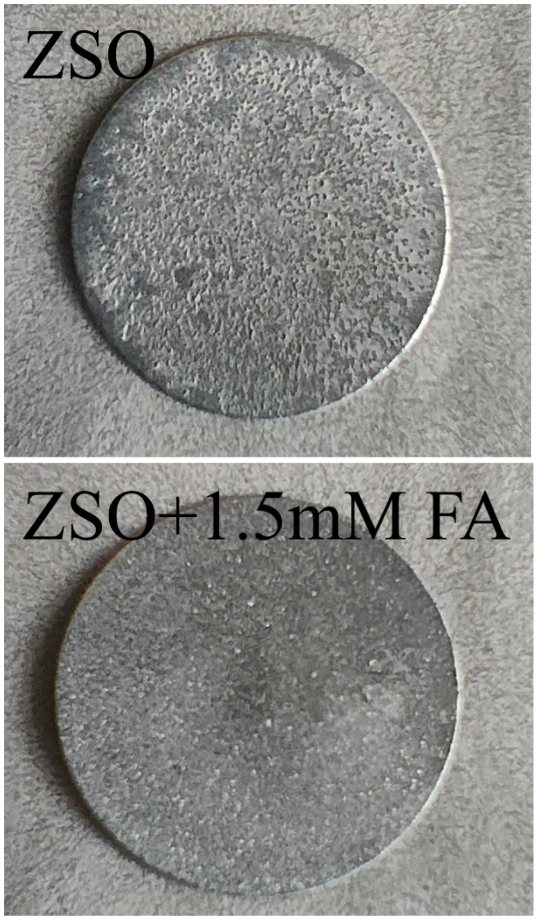

Figure S25: Images of cycled zinc anodes.

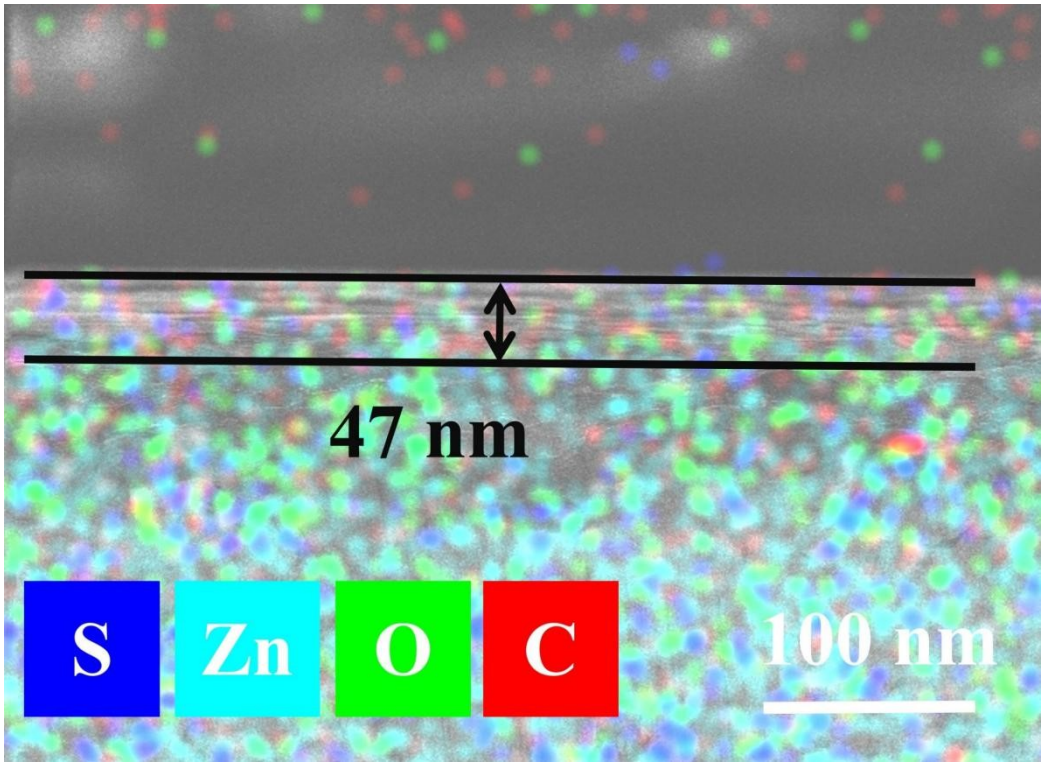

Figure S26: EDS spectrum of the SEI film.

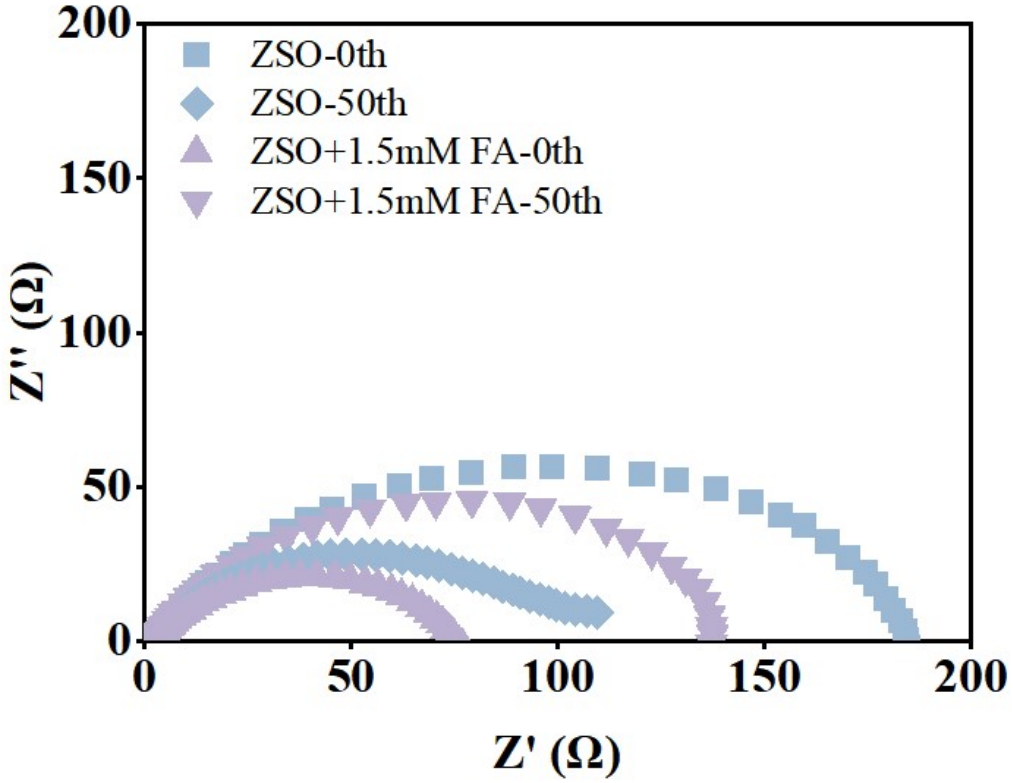

Figure S27: Impedance comparison before and after cycling.

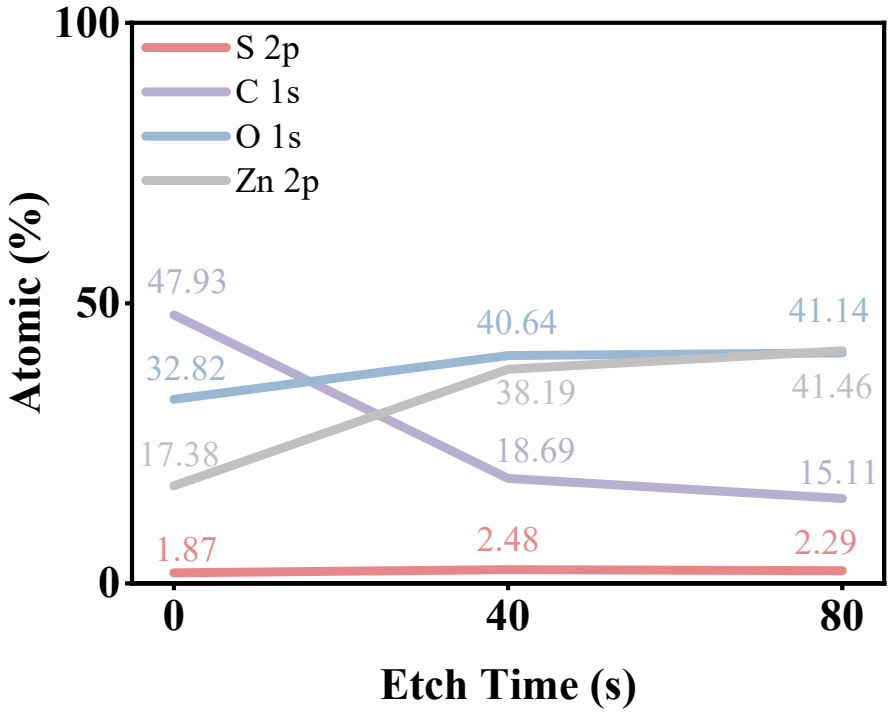

Figure S28: Elemental ratios at different sputtering depths.

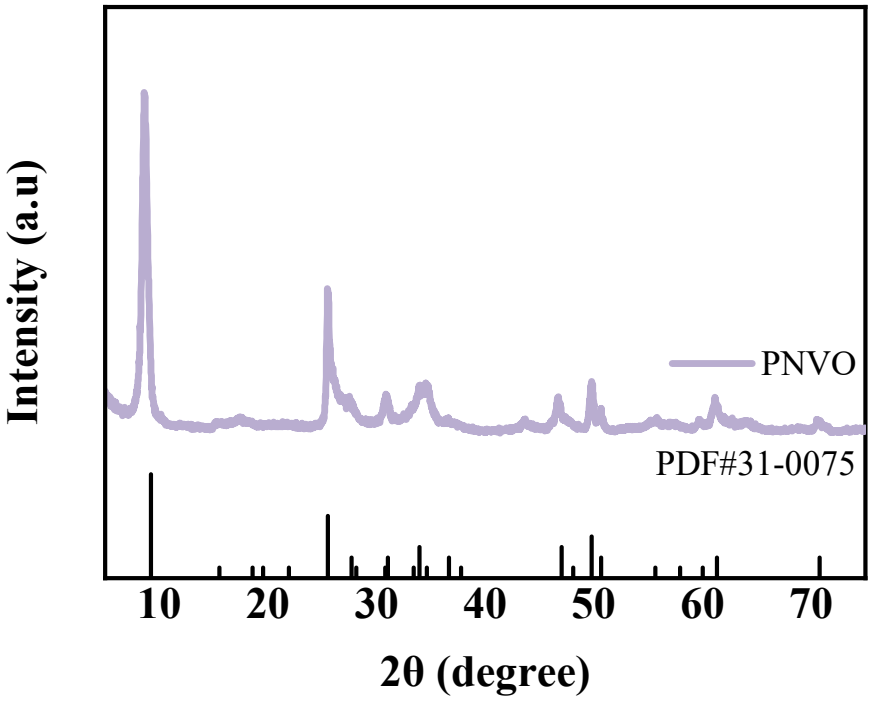

Figure S29: XRD pattern of P-$NH_4V_4O_{10}$.

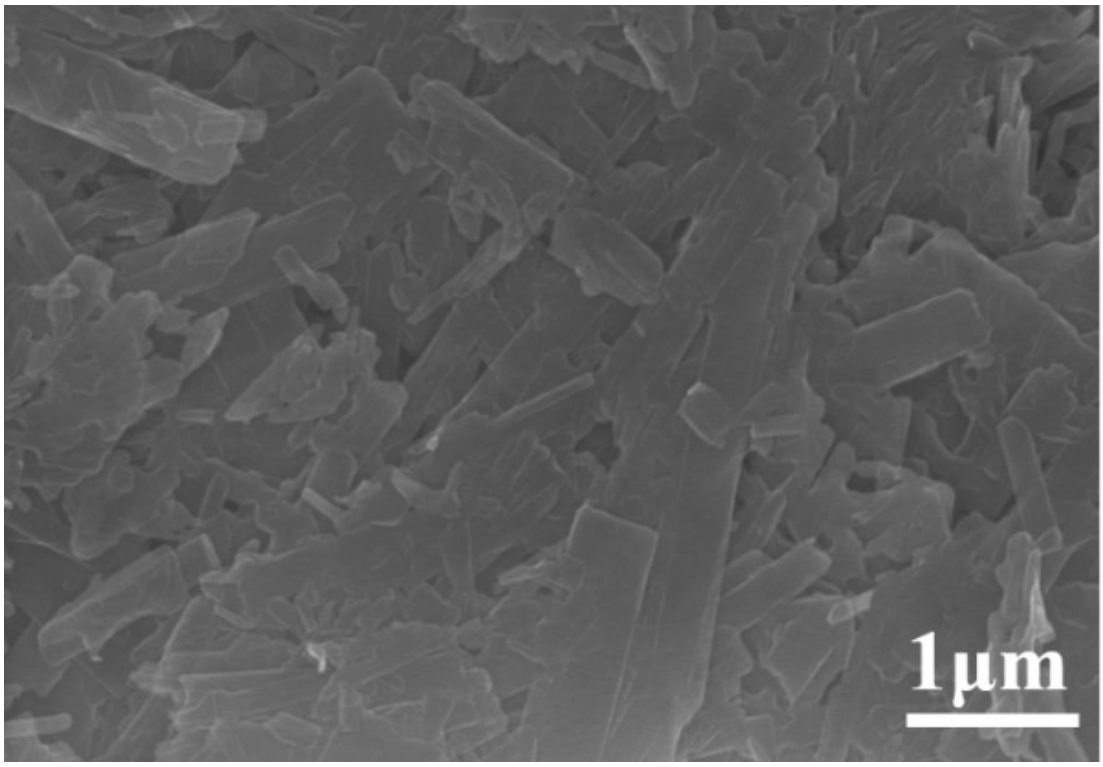

Figure S30: SEM image of P-$NH_4V_4O_{10}$.

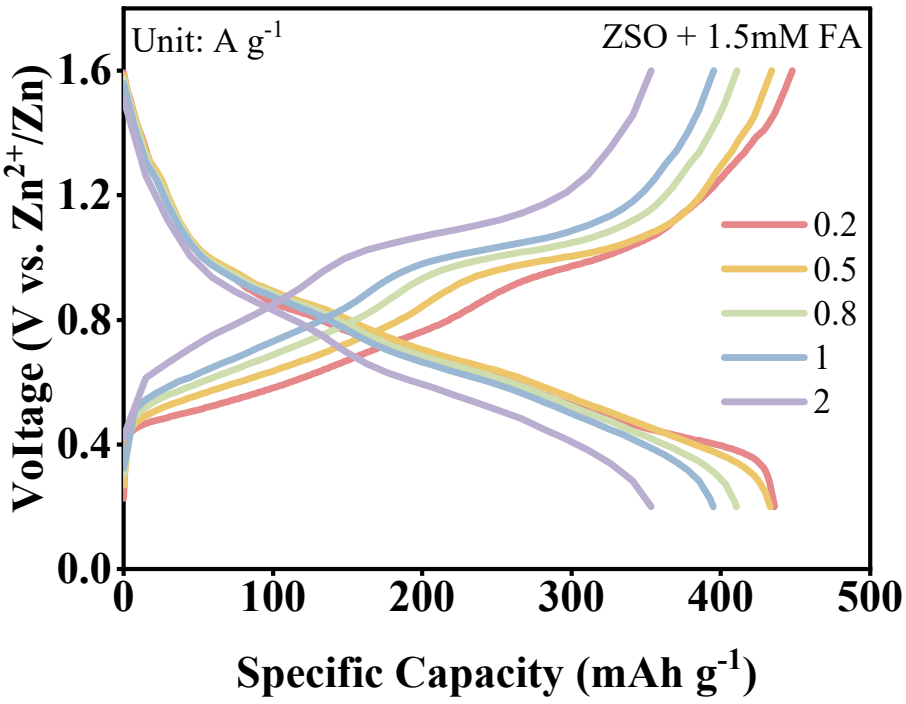

Figure S31: GCD curves of ZSO + 1.5 mM FA electrolyte.

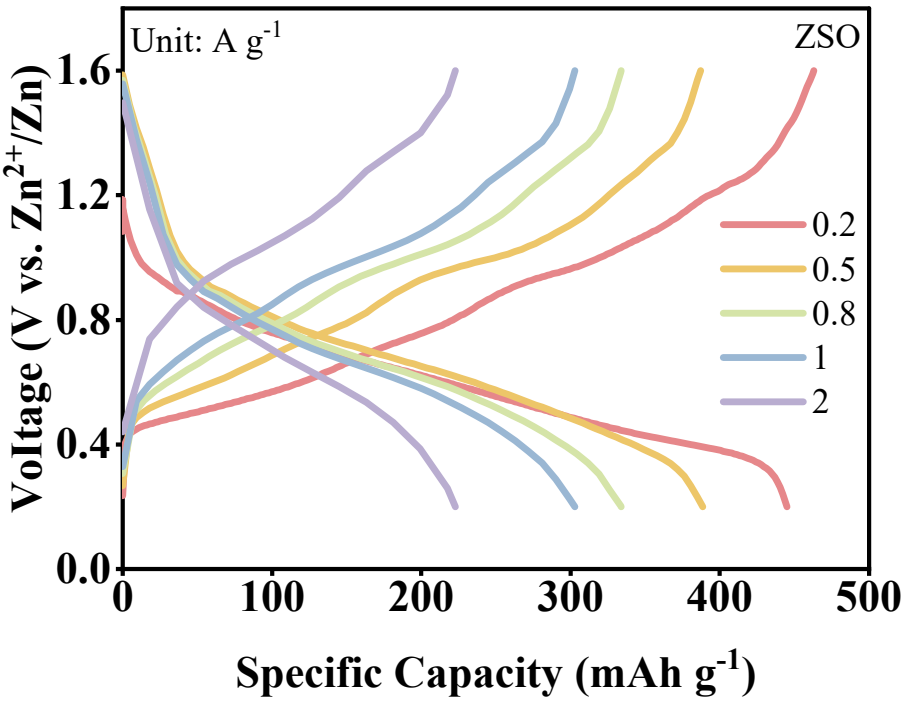

Figure S32: GCD curves of ZSO electrolyte.